Sensitive Protein Assay with Distinction of Conformations Based on Visible Absorption Changes of Citrate-Stabilized Gold Nanoparticles

ARTICLE *in* THE JOURNAL OF PHYSICAL CHEMISTRY C · APRIL 2009

Impact Factor: 4.77 · DOI: 10.1021/jp808405p

3 AUTHORS, INCLUDING:

Jashmini Deka
Sincrotrone Trieste S.C.p.A.
9 PUBLICATIONS **144** CITATIONS
SEE PROFILE

Anumita Paul
Indian Institute of Technology Guwahati
37 PUBLICATIONS **1,056** CITATIONS
SEE PROFILE

THE JOURNAL OF PHYSICAL CHEMISTRY C

Article

Sensitive Protein Assay with Distinction of Conformations Based on Visible Absorption Changes of Citrate-Stabilized Gold Nanoparticles

Jashmini Deka, Anumita Paul, and Arun Chattopadhyay

J. Phys. Chem. C, **2009**, 113 (17), 6936-6947• DOI: 10.1021/jp808405p • Publication Date (Web): 03 April 2009

Sensitive Protein Assay with Distinction of Conformations Based on Visible Absorption Changes of Citrate-Stabilized Gold Nanoparticles

Jashmini Deka,[†] Anumita Paul,*[,†] and Arun Chattopadhyay*[,†,‡]

Department of Chemistry and Centre for Nanotechnology, Indian Institute of Technology Guwahati, Guwahati 781 039, India

Received: September 22, 2008; Revised Manuscript Received: February 20, 2009

In this work, we introduce a new and potentially general method of assay of proteins in solution. In addition, the method could distinguish conformations of protein (native and denatured forms). The method is based on the changes in visible absorption spectra of citrate-stabilized Au nanoparticles (NPs) upon addition of a measured amount of protein. The behavior of four proteins, namely α-amylase, green fluorescent protein (GFP), amyloglucosidase (AMG) and bovine serum albumin (BSA) have been found to be different with respect to changes in the spectra of Au NPs. The spectral behaviors were also different between the native and denatured forms of the same protein. Interestingly, spectral changes in the presence of thiol-containing proteins (α-amylase and GFP) were different from those that either did not contain thiol at all or contained thiol that was not exposed to the solution (AMG and BSA). Transmission electron microscopic investigations revealed agglomeration of Au NPs in the presence of protein as the reason behind the change in absorption spectra. This has been further supported by dynamic light scattering based particle size analysis experiments. We have proposed a model based on the agglomeration of Au NPs in the presence of enzyme to account for the changes in the optical spectra. In addition, deconvolution analyses of the absorption spectra clearly indicated different levels of agglomeration for different proteins making the distinction possible.

Introduction

Proteins are one of the most important classes of biomolecules essential for life that are involved in virtually all functions of a cell. Proteins also hold a special place in biomimetic systems, where it can be used for biochemical synthesis, assembly, or other functions pertaining to their catalytic activities.[1−3] Understanding and appropriate use of their broad spectrum of functions require knowledge about the structures in native and denatured forms and the concentrations in vivo as well as in vitro. For example, proteomics play a central role in understanding and monitoring of various diseases such as Alzheimer's, heart diseases, and cancers.[4−7] This calls for development of highly sensitive methods for early detection of protein-related diseases and acquirement of extensive knowledge about the protein of interest. Fortunately, crystal structures of a large number of useful proteins are known.[8] In solution, not only is the knowledge of structure of the protein specific to its function important but also rapid quantification of its concentration is vital to its use in a medium. Conventional colorimetric methods for protein estimation, such as Biuret, Bicinchonic Acid (BCA), Lowry, and Bradford tests, use a sequence of steps involving reactions with optically sensitive molecules, followed by generation of calibration curves using bovine serum albumin (BSA) as a reference protein, which render them cumbersome. These methods, although useful, are not highly sensitive; the sensitivity range lying between 0.01 and 8.0 mg/mL, depending on the nature of the protein and the method used. However, modern experiments with ultra low quantities of biomaterials require development of newer methods—preferably using spectroscopic techniques—involving minimum number of chemicals and steps, for estimation of proteins in various reaction conditions, with possibly high sensitivity and specificity.

The advent of nanoscale science and associated technology brings newer opportunities in practicing biosciences that are unmatched by conventional means. For example, chemical and optical properties of inorganic nanoparticles (NPs) have been successfully employed in the field of biomedicine through sensing, drug delivery, and diagnostics.[9−13] The NPs have also been used in developing methods for identification and estimation of biomolecules,[14−16] and hence could be assumed to be potentially useful in proteomics as well. In this regard, surface plasmon resonance (SPR) of biocompatible Au NPs, with high optical extinction coefficient, has been found to be useful in developing NP-based diagnostics. For example, biofunctionalized Au NPs have been used for detection and quantification of proteins,[17−21] protein−protein,[22,23] and protein−membrane interaction studies[24] and separation of proteins.[25] Also, SPR of bulk Au film and self-assembled Au NPs have been employed in the quantification of denaturation of biomolecules,[26] and study of conformational changes of proteins.[27,28] Further, there are reports on the use of colloidal gold in the assay of proteins using the color change in a spot.[29,30] There is also a report of using colloidal gold to estimate bovine serum albumin (BSA) by measuring change in absorbance.[31] Further, binding of BSA to Au NPs has been studied by quartz crystal microbalance.[32] In addition, latex agglutination[33] and sol−gel aggregation[34] of functionalized latex as well as Au NPs have earlier been used for protein assay, although with moderate levels of sensitivity. Interestingly, notwithstanding the aforementioned developments in the field, quantification of protein in solution, taking advantage of the optical properties of nonfunctionalized Au NPs, remains largely unaddressed. The cited reports generally depend either on the conjugation of NPs with biomolecule for the

* To whom correspondence should be addressed. E-mail: anumita@iitg.ernet.in; arun@iitg.ernet.in.
[†] Department of Chemistry.
[‡] Centre for Nanotechnology.

10.1021/jp808405p CCC: $40.75
Published on Web 04/03/2009

recognition of antigen/protein of interest or modification of the biomolecule itself or use of low pH or polymer in increasing the sensitivity of the assay and are time-consuming. Thus, the development of a simple technique based on ordinary Au NPs (such as citrate stabilized Au NPs) in aqueous medium would be useful in quantitative and rapid estimation of proteins. The method would be even more versatile if identification of proteins as well as differentiation of their native versus denatured conformations could simultaneously be established.

Herein, we report the development of a new method for rapid and efficient quantification of proteins in aqueous solution based on changes in the SPR absorption of citrate-capped Au NPs in the medium. Addition of proteins to the medium containing citrate stabilized Au NPs led to broadening of the absorption spectrum, the area of which varied linearly over a range of concentration. That provided an easy way of estimation of concentration of a protein in the medium. However, beyond a critical concentration of the protein there was no change in the spectral behavior. Interestingly, the changes in spectral characteristics depended on the nature of the protein as well as its state. For example, α-amylase and green fluorescence protein (GFP), which contain free and exposed thiol groups in their native forms, led to changes in the spectra which were fundamentally different from those due to addition of amyloglucosidase (AMG) or bovine serum albumin (BSA) neither of which has any free and exposed thiol group in their native forms. Also, changes in the spectral characteristics of Au NPs were different for the native and denatured states for all of the proteins, thus providing an opportunity to distinguish between the two states in the medium. For example, while the native form of α-amylase led to significant change in the spectral behavior of Au NPs, the denatured form had little effect on the same. Transmission electron microscopic (TEM) measurements indicated that agglomeration of NPs in the presence of proteins was the primary reason for the optical behaviors; the larger was the extent of agglomeration the larger was the change in the absorption spectra of Au NPs. Also the extent of agglomeration was dependent on the concentration and nature of proteins. The results were further substantiated by dynamic light scattering (DLS) based measurement of particle sizes. In order to account for the changes in the absorption spectra, we have proposed a model based on the agglomeration of Au NPs in the presence of proteins. In the analyses, deconvolutions of the spectra clearly indicated the appearance and subsequent increase of absorption due to agglomerated state at the expense of the unagglomerated one. Overall, the method provided a new way of estimation of proteins in solution with the ability to distinguish between the nature of proteins and the state of the proteins, where the sensitivity is similar to other NP-based estimation. Also, the method allowed estimation of protein with as low of a concentration as 2.0 ng/mL, thus providing a quick and easy assay of proteins with high sensitivity.

Experimental Section

Materials. ***Preparation of Citrate Stabilized Au NPs.*** Au NPs were prepared by a known method of citrate reduction of $HAuCl_4$.[35,36] A 250.0-μL portion of 1.73×10^{-2} M $HAuCl_4$ (Sigma- Aldrich Chemical Co.) was added to 10.0 mL of MilliQ grade water and then heated to boiling. Then 400.0 μL of 0.2 M trisodium citrate 2-hydrate (Merck) was added to the boiling solution (all at once) and the boiling (or refluxing) was continued for another 15 min to ensure complete reduction of $HAuCl_4$. The solution turned deep red, indicating the synthesis of Au NPs. The red solution so obtained was cooled to room temperature; the volume was adjusted to 10.0 mL and finally was diluted 4× with phosphate buffer of pH 7.0 for further use.

Preparation of Enzyme/Protein Solution. A 1.0-mg/mL portion of enzyme/protein solution was prepared by dissolving the solid protein in appropriate buffer—phosphate buffer of pH 7.0 for α-amylase (from hog pancreas, Fluka), GFP and BSA (SRL) and acetate buffer of pH 5.0 for AMG (from *Aspergillus niger*, Fluka) was used. This was further diluted 10× to obtain 0.1 mg/mL protein solution. It was observed that α-amylase was sparingly soluble in buffer solution (pH 7.0). Hence, the 1 mg/mL α-amylase solution was stirred for 20 min for better mixing. This was followed by centrifugation at 5000 rpm for 20 min. The supernatant was collected and used for further analysis. It was also observed that the amount of protein present in the final solution thus prepared was much less than 1 mg/mL (as discussed later). GFP (wild type) was isolated and subsequently purified from overnight grown culture of GFP expressing *E. coli*.[37] This is followed by lyophilization and the dried protein was weighed for further sample preparation.

Preparation of Denatured Enzyme/Protein Solution. A 3.0-mL portion of the 0.1 mg/mL of enzyme/protein solution, prepared as discussed above, was kept in a water bath at 80 °C for 30 min. The volume was made up for the loss due to evaporation and the solution was then used for further analysis.

Estimation of Protein Content in the 1.0 mg/mL Enzyme/Protein Solution. The actual protein content was calculated using the standard Bradford test[38] for protein for 1.0 mg/mL enzyme/protein solution. It was observed that the tests were carried out within the linear region of estimation using Bradford method.[39] This was used as a reference for calculating the amount of protein in the volume of enzyme solution used in further analyses. However, since BSA was the standard protein taken as reference in the Bradford test and GFP was obtained as pure, the absolute amount of both the enzymes taken was considered as it is for further calculations. It is important to mention here that in the Experimental Section the concentrations of enzyme/protein refer to are as prepared concentrations, whereas in the Results and Discussion (as well as Supporting Information) section the exact concentrations of them as estimated by Bradford test are mentioned. Further, since the enzyme/protein (especially sparingly soluble α-amylase) may contain stabilizers which might interfere with the Bradford test, it is best to carry out the estimation of concentrations where serial dilutions would result in linear behavior with respect to the test. Sample test for the linear change in absorbance of the probe dye (λ_{max} = 595 nm) as a function of α-amylase concentration is shown in Figure S1 (of the Supporting Information). The calibration of the concentration of α-amylase measured using the present method has been performed using Bradford test in the linear region of absorbance change.

Successive Addition of Enzyme/Protein Solution to Citrate-Capped Au NPs. A 3.0-mL portion of the Au NP solution was taken in a cuvette, and the UV−vis spectrum was recorded (using a Hitachi U-2800 spectrophotometer). A 20.0-μL portion of 0.1 mg/mL solution of the enzyme/protein (α-amylase) was added to it, shaken well, and again the UV−vis spectrum was recorded. This was followed by the addition of 30.0 μL of protein solution followed by recording of UV−vis spectrum. Protein addition was continued (by adding 30.0 μL solution each time) followed by recording of UV−vis spectrum, till a saturation was achieved in the spectra. However, in the case of AMG, BSA and GFP, enzyme/protein solution was added in an increment of 10.0 μL. All of the UV−vis spectra were recorded immediately after addition of protein. All of the peak

areas were then calculated (after performing proper volume correction) and plotted against the concentration of the protein in the solution.

Calculation of the Area under the UV−vis Spectrum. This was performed automatically by the software associated with the data acquisition of the spectrophotometer. The area was calculated by joining a line between two points in the absorption spectrum encompassing the area above the line and the absorption spectrum (graph). For α-amylase, the extreme wavelengths were set at 405 and 650 nm, whereas that for GFP and AMG were set at 405 and 750 nm and for BSA they were at 425 and 750 nm. A typical view of such area is shown in the Supporting Information (Figure S2). All of the spectra were normalized to incorporate the dilution factor in the calculation of area. There was thus no need for additional baseline subtraction.

Sample Preparation for TEM Analysis. Solution-containing Au NPs (before enzyme addition) and those of Au NPs in the presence of 0.03 and 0.06 mL α-amylase solution (each containing 0.1 mg/mL) were drop cast onto Cu grids (right after enzyme addition and UV−vis analyses) and then left for air drying overnight. These grids were further analyzed by a Jeol 2100 TEM machine (operated at a maximum voltage of 200 kV). Similarly for the preparation of TEM samples with BSA (native and denatured) 0.03 and 0.16 mL of protein solution (each containing 0.1 mg/mL) were added to 3 mL of Au NP solution followed by drop-casting on the grid.

Particle Size Analysis by DLS Method. An 18.0-mL portion of the Au NP solution was taken in a cell for which particle size distribution was measured using a Horiba LB-550 instrument. To this, 0.120 mL of 0.1 mg/mL α-amylase solution was added and shaken well before recording the particle size distribution again. The analysis was continued up to an addition of total of 1.38 mL α-amylase solution in the same cell. The particle size distribution was recorded after each addition. The ratios of enzyme to Au NPs were kept the same as in the other experiments.

Results and Discussion

Upon addition of a microgram quantity of any of the four proteins, namely α-amylase, AMG, GFP, and BSA in their native forms, into ruby red colored citrate-capped Au NP solution, the color changed to purple. The intensity of the color increased upon addition of further quantities of protein. However, there was no change observed after a certain concentration of the protein was added. Also, the distinction between changes in color due to different proteins could not be made with naked eye. Similar observations were made with the denatured proteins. UV−vis spectra of Au NPs upon addition of any of the proteins broadened, accompanied by small red-shifts in the maxima. However, for the sake of clarity, spectral characteristics due to addition of each protein would be presented separately in the following sections.

When 0.02 mL of 3.3 μg/mL solution of native α-amylase was added to 3.0 mL of the citrate-stabilized Au NP solution, the absorption maximum shifted from 522 to 524 nm (Figure 1A). There was also significant broadening of the peak, which is clear from the figure. The change in the spectral characteristics continued to occur upon further addition of the protein. However, at a concentration of 0.134 μg/mL of protein and above, there was no change in the spectra indicating saturation in the observed effect. Interestingly, when similar experiments were carried out with denatured α-amylase, the changes in the spectra of the Au NPs were rather small (Figure 1B). Although the intensity of absorption changed discernibly, broadening of the spectra was rather small. A plot of the total area under the spectrum (details of calculation provided in the experimental section), shown in Figure 1C, was found to vary linearly with the concentration of native protein up to 0.106 μg/mL. At above that concentration, the change in area was small and gradually reached saturation at 0.134 μg/mL. However, the change in the area versus concentration of the denatured protein was less significant in comparison to that of the native form of the protein. Although, there was a linear increase in the area with concentration the slope was significantly smaller than that of the native form (Figure 1D). Interestingly, the changes—albeit small—continued to occur at higher values of protein concentrations in comparison to that of the native form. For example, while the linearity was maintained till a concentration of 0.106 μg/mL of the native protein, the same could be observed for the denatured form at a concentration up to 0.337 μg/mL. The above results indicate that interactions of α-amylase with citrate stabilized Au NPs is dependent not only on the concentration of the protein but also on its (native versus denatured) tertiary structures. Thus, changes in the absorption characteristics of citrate-stabilized Au NPs have the kernel of a method for simultaneous estimation of protein concentration as well as obtaining knowledge of its tertiary structure in solution.

Further investigations by TEM measurements indicated agglomeration of Au NPs in the presence of native form of the protein. The results are shown in Figure 2. Figure 2A shows the image of citrate-stabilized Au NPs produced in the present method and in the absence of any protein. The particles produced were monodispersed in size and spherical in shapes. Also, the average particle size was calculated to be 7.4 nm ± 1.1 nm. Addition of 0.03 mL of 3.3 μg/mL α-amylase solution to 3.0 mL Au NP solution led to apparent aggregation of the NPs without affecting their size (Figure 2B). However, there were significant numbers of particles that were not aggregated, as is clear from the figure. Upon further addition of the protein (0.06 μg/mL protein), the network of the Au NP assembly grew further which is clear from Figure 2C. In other words, at higher concentrations of protein, the size of the assembly as well as the percentage of particles involved in the assembly formation increased. It is also interesting to note that addition of denatured proteins did not lead to significant agglomeration even at higher concentrations of proteins. A typical image is shown in Figure 2D, which clearly shows that almost all of the particles remained largely separated even at a concentration of 0.06 μg/mL. The agglomeration induced by the native proteins of the same concentration was substantial (Figure 2C). Particle size distribution analysis recorded by DLS method also indicated agglomeration of NPs in the presence of native protein. For example, the average particle size of citrate stabilized Au NPs was found to be 33.9 ± 3.4 nm. Upon addition of 0.02 μg/mL of the native protein there was no significant change in the hydrodynamic diameter. However, the average size was 1.56 ± 0.15 μm upon addition of 0.05 μg/mL of the protein, which changed to 1.77 ± 0.17 μm when the concentration was 0.11 μg/mL. The sizes did not change significantly upon further addition of proteins. The details of the results of DLS measurements are given in the Supporting Information (Figure S3). Further, dilution experiments suggest that agglomeration of the NPs in the presence of native protein was irreversible. For example, when the Au NP solution containing 0.08 μg/mL of native protein was diluted to 1.5× that of the original volume, there was no change in the shape of the absorption spectrum (Figure S4 of the Supporting Information). In other words,

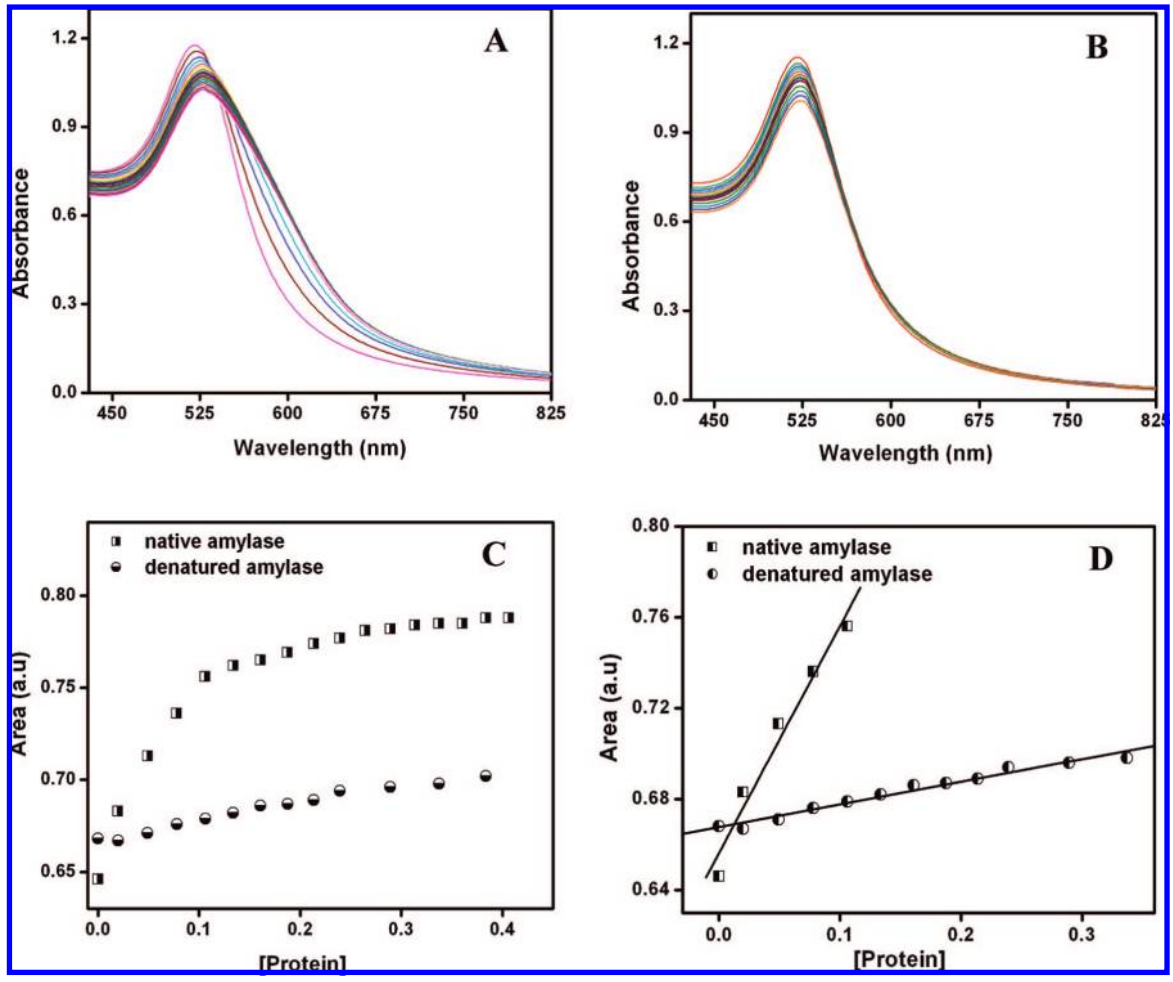

Figure 1. (A) UV−vis spectra of Au NPs with various amounts of native α-amylase added successively (0.02 μg/mL to 0.41 μg/mL of final protein concentration). (B) UV−vis spectra of Au NPs with various amounts of denatured α-amylase added successively (the successive concentrations were the same as in A). (C) Area under the curve versus the corresponding protein concentration (in μg/mL) for native and denatured α-amylase. (D) The linear region of the graphs in C.

dilution of the protein containing Au NP dispersion did not lead to systematic changes in the absorption spectra. Also, the agglomerated composite of protein and NPs was quite stable with respect to volume dilution.

In order to understand whether agglomeration of Au NPs by native α-amylase was consequential due to addition of successive amounts of proteins or not, the following experiment was carried out. Ten 3.0 mL Au NP solutions were taken from the same stock solution and kept separately in test tubes. To each of the test tubes, different amounts of α-amylase were added and the final concentrations of proteins were the same as those corresponding to the graphs in Figure 1A (0.02 μg/mL, 0.04 μg/mL, 0.06 μg/mL, etc.). However, the final concentrations were adjusted with addition of an even smaller amount of proteins in several portions (in multiples of 0.002 μg/mL) and UV−vis spectra of all the solutions were recorded. The UV−vis spectra and the corresponding area versus protein concentration plot are shown in Figure S5 of the Supporting Information and Figure 3A respectively. As is clear from the graphs, the results are identical to those obtained using sequential addition (Figure 1, parts A and C). Also, it is important to mention here that the lowest concentration of protein that induced changes in the absorption spectrum of Au NPs was found to be 0.002 μg/mL. The above results led to three essential conclusions. The first is that the effect of native α-amylase on the spectrum of Au NP solution is dependent on the concentration of protein and not

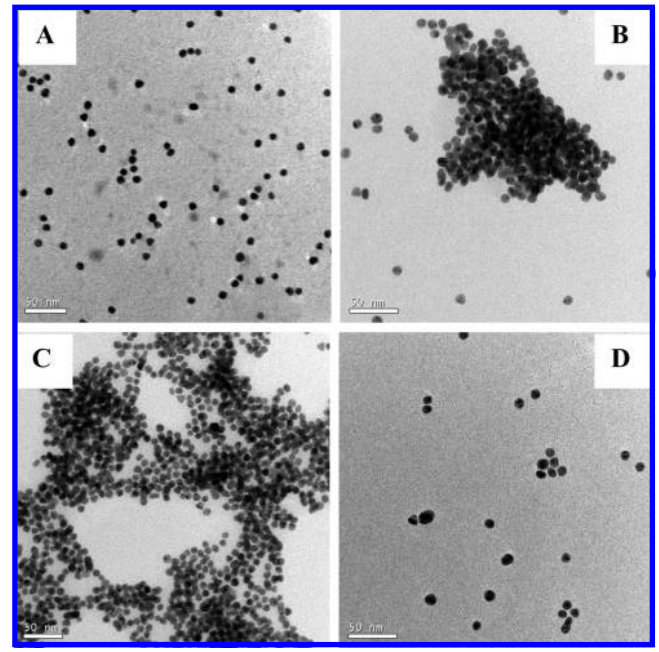

Figure 2. TEM images of (A) citrate stabilized Au NPs, (B) Au NPs in the presence of 0.03 μg/mL of native α-amylase, (C) Au NPs in the presence of 0.06 μg/mL of native α-amylase, and (D) Au NPs in the presence of 0.06 μg/mL of heat denatured α-amylase. Scale bar is 50 nm in all.

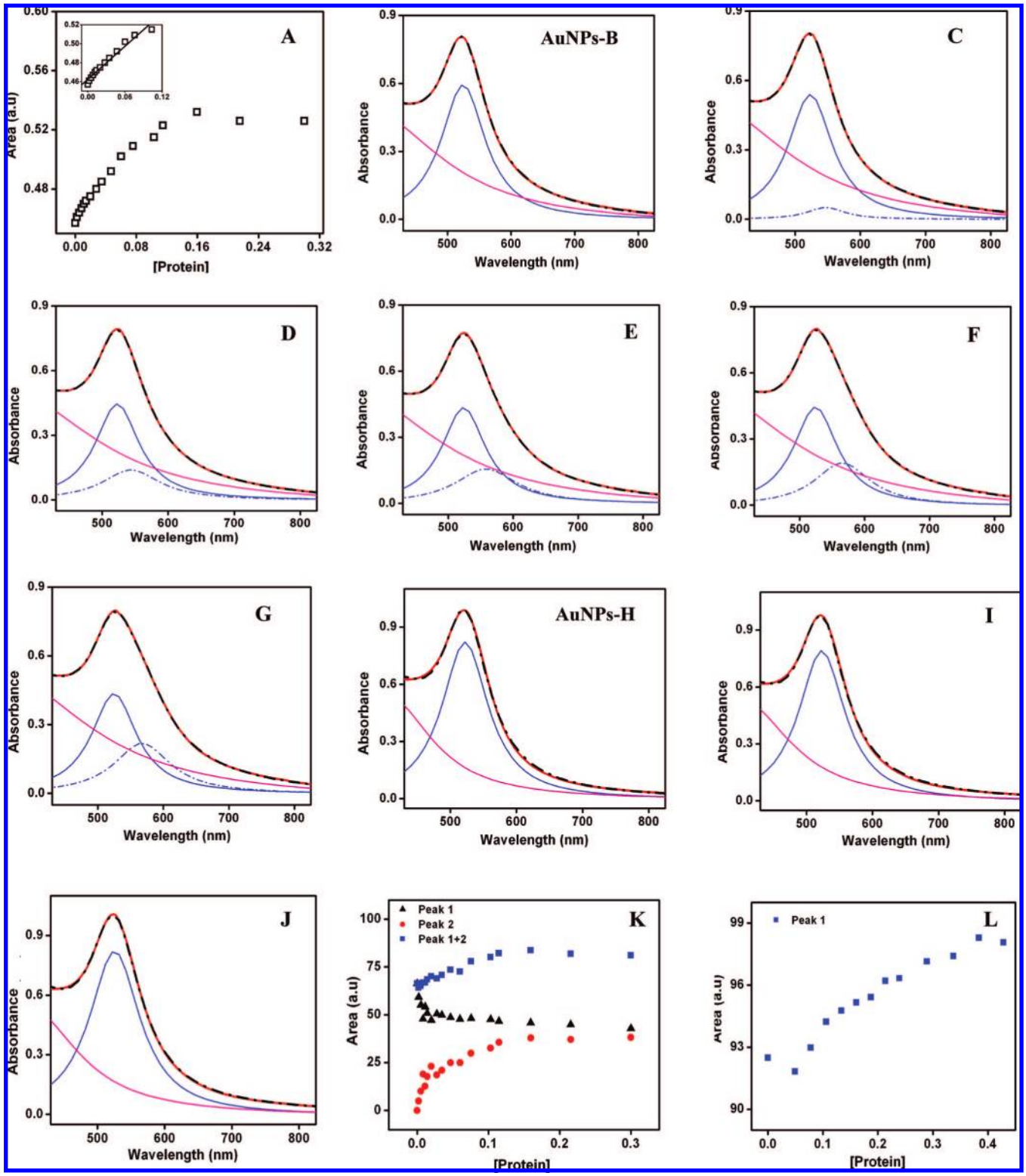

Figure 3. (A) Area (under the curve) versus protein concentration (in μg/mL) plot for (native) α-amylase addition to Au NPs in small increments (inset shows the linear region). (B) Deconvoluted curves of Au NPs only used for native amylase. (C−G) Deconvoluted curves of Au NPs in presence of 0.002, 0.005, 0.075, 0.16, and 0.3 μg/mL respectively of protein (native enzyme). (H) Deconvoluted curves of Au NPs only used for denatured enzyme. (I−J) Deconvoluted curves of Au NPs in presence of 0.02 μg/mL and 0.43 μg/mL of protein (denatured enzyme). Area (under the curve) versus protein concentration (in μg/mL) plot for the same set for all the peaks obtained after deconvolution of the UV−vis curves of (K) native α-amylase and (L) denatured α-amylase. The red curves shown in graphs B−J are the experimental curves and the dotted black lines show the Lorentzian fit achieved after deconvolution. The solid blue curves represent the 1st peak and the dotted blue ones are the 2nd peak. The curves in pink are baselines.

on the mode of addition (sequential addition versus addition at once). Second, the spectroscopic absorption changes of Au NPs can be the basis of quantitative estimation of native α-amylase in solution. Third, the lowest concentration of α-amylase that can be estimated is 40 picomolar (2 ng/mL), which is much less than that obtained from the methods commonly used for

the estimation of proteins in solution. Thus the method is not only simpler and easy to execute but also more sensitive than the conventional ones. Of course, the ability to differentiate between the native and denatured form of the protein is an additional advantage of the present method over others.

For a colloidal solution with N particles per unit volume the extinction of light could be written as follows:[40]

$$A = \log_{10}\frac{I_o}{I} = \frac{NQ_{ext}l}{2.303} \quad (1)$$

Here, I_0 and I are the intensities of incident and transmitted light, l is the path length and Q_{ext} is the extinction coefficient of a single particle.

For very small metal particles, the absorption of light could be explained based on Mie scattering theory and the extinction coefficient can be written as,[40]

$$Q_{ext}(\lambda) = \frac{24\pi^2R^3\varepsilon_m^{3/2}}{\lambda}\frac{\varepsilon''}{(\varepsilon' + 2\varepsilon_m)^2 + \varepsilon''^2} \quad (2)$$

Here, R is the radius of the spherical NP, λ is the wavelength of the light, ϵ_m is the dielectric function of the medium, ε' and ε are the real and imaginary parts of frequency dependent dielectric function (ε) of the NP ($\varepsilon = \varepsilon' + i\varepsilon''$).

However, when the particle is coated by a layer of organic or inorganic material with different dielectric constant, the extinction coefficient of the particle can then be written as,[27,40]

$$Q_{ext}(\lambda) = \frac{8\pi^2R^3(\varepsilon_m)^{1/2}}{\lambda} \times \mathrm{Im}\left\{\frac{(\varepsilon_2 - \varepsilon_m)(\varepsilon_1 + 2\varepsilon_2) + (1-g)(\varepsilon_1 - \varepsilon_2)(\varepsilon_m + 2\varepsilon_2)}{(\varepsilon_2 + 2\varepsilon_m)(\varepsilon_1 + 2\varepsilon_2) + (1-g)(\varepsilon_1 - \varepsilon_2)(2\varepsilon_2 - 2\varepsilon_m)}\right\} \quad (3)$$

Here, $\varepsilon_1$and ε_2 are the complex dielectric functions of the particle core and the surface coating, and g is the volume fraction occupied by the surface coating. Thus, the extinction of light not only depends on the dielectric property of NPs but also of the surface coating and the medium. When the protein is added to citrate stabilized Au NPs in aqueous medium, it might get completely or partially attached to the NPs replacing the citrates. At lower concentrations of the protein, the broadening that is observed could be due to change in the dielectric constant of the coating because of attachment of the protein. However, at higher concentrations, agglomeration of the proteins attached to the Au NPs as well as the excess ones occur. This leads to significant change in the dielectric constant of the coating as well as the immediate vicinity of the medium. Thus, broadening becomes very pronounced. In addition, interaction between the NPs in close proximity in the agglomerated state would lead to broadening and red-shifting of the peak. This could be accounted for by the change in value of R in eq 3. We propose the following model to account for the changes in the spectra and to calculate the protein concentration-dependent absorbance of the Au NPs.

The agglomeration of NP and protein could be written in the following way.

$$n\mathrm{Au_{NP}} + m\mathrm{Enz} \rightarrow (\mathrm{Au_{NP}})_n(\mathrm{Enz})_m \quad (4)$$

Here, n is the number of NP and m is the number of enzyme molecules involved in the agglomerated composite formation. At lower concentrations of enzyme, when agglomeration is not significant, there would be two kinds of species that would lead to extinction of light—the unagglomerated Au NPs and agglomerated Au NP—enzyme composite. Thus, the total extinction of light could be rewritten as follows:

$$A(\upsilon) = Q_{ext_{NP}}(\upsilon)C_{NP}l + Q_{ext_{comp}}(\upsilon)C_{comp}l \quad (5)$$

Here, the subscripts represent the species and C represents concentration of a particular species and l is the length of the cuvette (cell). Equation 5 could be written in terms of absorption as follows:

$$A(\upsilon) = A_{NP}(\upsilon) + A_{comp}(\upsilon) \quad (6)$$

Here, $A(\nu)$ is the frequency dependent total absorption, and $A_{NP}(\nu)$ is that due to unagglomerated NP and $A_{comp}(\nu)$ is that due to composite. While there are reports of change in intensity of absorption and shift in peak position as measures of changes due to agglomeration of NP, a better and more comprehensive one would be related to oscillator strength, which is related to total area under the absorption spectrum. One can then write eq 6 as,

$$\int A(\upsilon)d\upsilon = \int A_{NP}(\upsilon)d\upsilon + \int A_{comp}(\upsilon)d\upsilon \quad (7)$$

One can also express eq 7 in terms of integration over wavelengths (λ),

$$\int A(\lambda)d\lambda = \int A_{NP}(\lambda)d\lambda + \int A_{comp}(\lambda)d\lambda \quad (8)$$

Thus, the total area under the experimental absorption spectrum could be interpreted as superposition of spectra due to unagglomerated Au NPs and agglomerated NPs. The changes in the area would reflect changes in the concentration of both the species. In the present set of experiments, the changes were observed in terms of primarily spectral broadening, while in some instances accompanying red-shift in peak could be observed—albeit small. This made the comparison of absorption spectra of unaffected Au NPs and agglomerated Au NPs as such not possible. However, appropriate deconvolution of the spectra could be performed to discern the effect of agglomeration of the protein and NPs, in a more quantitative manner. In order to account for broadening of peak, each UV−vis spectrum was deconvoluted using Lorentzian peak fitting routines available in standard commercial graphics software packages. Also, the Lorentzian fit after several iterations matched well with the absorption spectra with R^2 values better than 0.99. We have used commercially available software (Microcal Origin 7.0) for the analyses. The experimental spectra were deconvoluted and fitted by the nonlinear curve fitting method using software in-built Lorentzian function. Multiple (two to five) peaks were used to get good fit by iterative methods. It was observed that the area of the peaks obtained after deconvolution were little affected by the choice of the number of baselines chosen to fit the curves. For example, in the case of GFP, the areas of peaks 1 and 2 remained nearly the same when the data were fitted to one baseline and two peaks instead of two baselines and two peaks (Figure S8 of the Supporting Information). However,

regression factors of curve fitting with lesser numbers of baselines were poorer in the region outside the peak due to Au NPs, i.e., below 450 nm and above 650 nm, which consist of background extinction. Four examples are shown in Figure S7 of the Supporting Information. Hence, it is probably reasonable to conclude that the present method of peak analysis works well for the observed spectra and can be used in general. The results corresponding to addition of native α-amylase are shown in Figure 3. As is clear from Figure 3B, the initial solution consisted of a single peak at 522 nm (along with a background) corresponding to that of Au NPs in citrate solution. When 0.002 μg/mL of protein was added to the solution, the intensity of the peak at 522 nm decreased significantly, while a second peak at 542 nm appeared (Figure 3C). Further addition of proteins decreased the intensity of the peak at 522 nm. However, the peak at higher wavelength not only increased in intensity, but also the wavelength maximum red-shifted increasingly with concentration (Figures 3D to 3G). These results indicate that with addition of the protein, the agglomeration takes place and continues to increase with the concentration of protein. However, even in the agglomerated state, the peak due to original Au NPs does not completely vanish, indicating that isolated Au NPs were present in significant numbers even in the agglomeration. In other words, addition of protein might not have removed the citrate cover to the NPs completely. However, proteins may lead to agglomeration of citrate stabilized NPs. Aggregation of the Au NPs is also known to be induced by London/van der Waals attractive forces between the nanoparticles.[41,42] Proteins contain various amino acid residues on their surfaces, which can lead to charge neutralization by interacting with citrate and thus leading to agglomeration of the NPs. Amino groups, such as lysine and histidine, are known to show strong electrostatic interaction with citrate capped Au NPs. Further, it is plausible that even in the agglomerated composite there could be individual NPs that do not interact with each other electrostatically to give rise to a second peak and hence contributes to the intensity of the peak at 522 nm (i.e., unagglomerated Au NP). Interestingly, when denatured protein (α-amylase) was added to the Au NP solution there was no appearance of the second peak (Figure 3H−J), indicating lack of agglomeration. This is consistent with the observation of TEM measurements. A plot of area of the component peaks versus concentration of protein (Figure 3K) indicates that for the addition of native protein, the area of the peak at 522 nm decreased linearly up to a protein concentration of 0.106 μg/mL, while the area of the peak at higher wavelength increased linearly up to the same concentration. Both areas leveled off above this concentration of protein. Also, the summation of the two areas at different protein concentration increased linearly up to the protein concentration of 0.106 μg/mL and then leveled off, similar to the experimental observations (Figure 3L). However, in the case of denatured protein, the area of the peak at 522 nm hardly changed, indicating that the denatured protein did not lead to significant changes in the spectral characteristics of Au NPs. Thus, from both the experimentally observed spectra and their deconvolutions, it is clear that changes in the absorption characteristics of Au NPs could be used to estimate the concentration of native α-amylase (up to an upper limit of 0.106 μg/mL), where the area of the absorption increases linearly with the concentration of the protein. Alternatively, the same experiments could be used to distinguish between the native and denatured form of the protein in solution.

Interestingly, addition of GFP to the citrate stabilized Au NP solution also led to observations of optical behavior similar to those with α-amylase. For example, broadening of the absorption spectrum was observed upon addition of the native protein. However, the effect was pronounced at higher concentrations of the protein in comparison to that of α-amylase. For example, the linear region of spectral broadening of area was observed up to a protein concentration of 1.639 μg/mL (Figure 4A,B), which was much higher than that of α-amylase. Also, the broadening of spectra was less pronounced in the denatured protein (Figure 4A,B). In other words, the changes were much sharper with the native form than the denatured form of the protein. This is also similar to those observed in case of α-amylase. However, the changes in the case of denatured GFP were more significant than that due to the presence of denatured α-amylase. The details of absorption spectra changes upon addition of native and denatured GFP are shown in the Supporting Information (Figure S6). Interestingly, there is an isobestic point in the absorption spectra associated with both the native as well as denatured protein, occurring at 535 and 540 nm respectively. This possibly indicates conversion of individual Au NPs into agglomerated form in the presence of protein, while the shift in peak due to agglomeration is more prominent than those involved with α-amylase. Further, the lowest concentration of the native as well as denatured form of GFP that induced changes was 0.332 μg/mL. Deconvolutions of the spectra of Au NPs associated with both the native and denatured form of the protein indicate behavior similar to those of α-amylase (Figure S7 of the Supporting Information). The original peak due to unagglomerated protein decreased gradually, while the peak due to agglomeration increased gradually up to a concentration of 1.639 μg/mL for the native protein. Similar results were observed for the denatured one; however, the changes were less dramatic as can be seen from the figure. The combination of decrease in the area of the graph due to unagglomerated Au NPs only and increase in the area of the agglomerated Au NPs spectra could account for the observed changes in the experimental spectra (Figure 4C,D).

The three-dimensional native structure of α-amylase in solution consists of two cysteine thiol groups that are exposed to the medium, which are known to covalently bind to Au NPs.[43,44] However, native GFP in solution consists of a tertiary structure that has one cysteine thiol group that is exposed to the medium. Since Au NP is known to have strong affinity for thiol group that forms Au−S bond on the surface of the NP, it is plausible that for both the proteins—in their native forms—thiol groups are involved in the formation of agglomeration. One cannot, however, exclude the role of other amino acids that could interact with the NPs electrostatically. Overall, the interactions of the NPs with the proteins might be similar and that could involve changes in the tertiary structure of the protein, leading to agglomeration. Alternatively, the proteins in the denatured form need not have the thiol group exposed to the medium; it might be buried in the structure and may not be available for bonding with the NPs. This would mean that the interaction would primarily be electrostatic that might not necessarily lead to significant agglomeration of the protein and Au NPs. This could be the reason for the differences that has been observed with respect to interactions of the native and denatured forms of the proteins with Au NPs. However, the role of hydrophobic forces in the denatured conformations of the proteins may play a significant role in determining the interactions with the citrate stabilized NPs and consequently the changes in the spectra.

Further experiments with AMG showed significant broadening of spectra of Au NPs in the presence of both native and denatured proteins (Figure S9 of the Supporting Information).

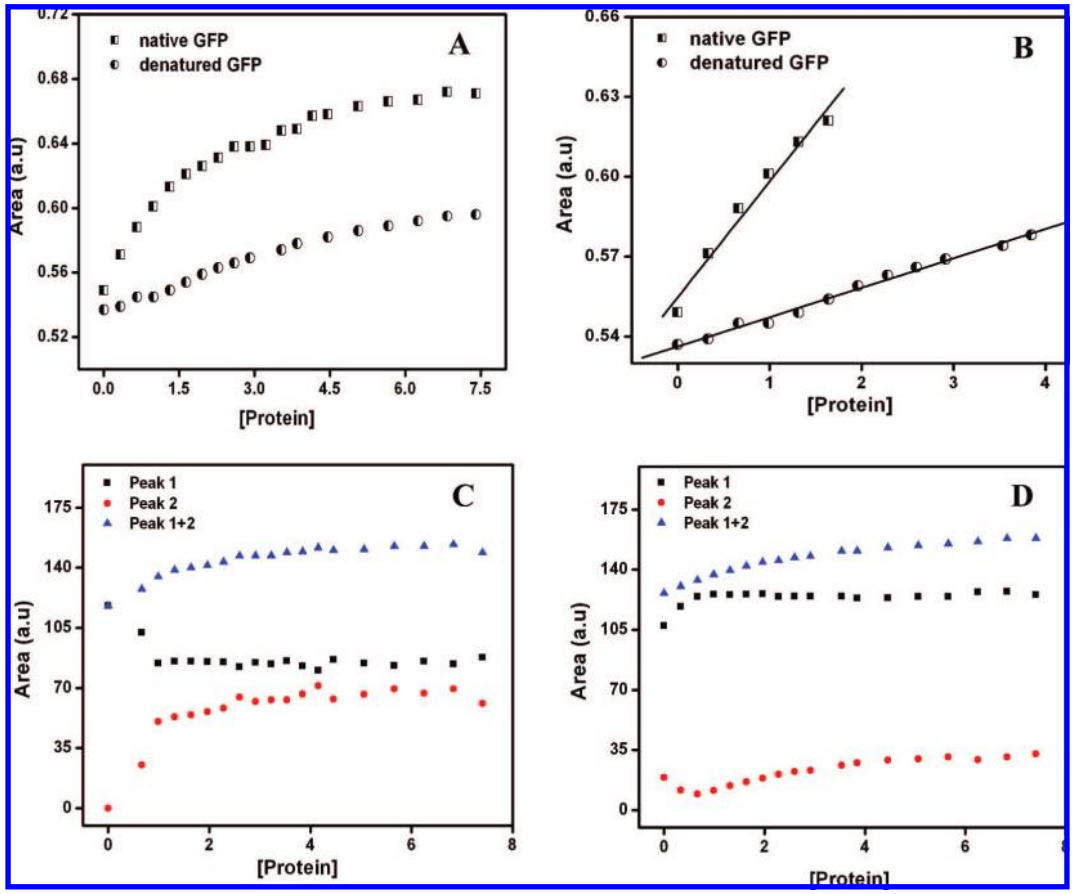

Figure 4. (A) Area under the graph versus the corresponding protein concentration (in μg/mL) for native and denatured GFP. (B) The linear region of the graphs in A. The peak areas of all the component peaks and their summation against the protein concentration (in μg/mL) obtained by deconvolution for (C) native GFP and (D) denatured GFP.

There were also significant decreases in intensity of absorption maxima for both the samples. However, a shift in the absorption maximum was more prominent in the samples consisting of denatured proteins than those containing native forms. The areas under the absorption spectra increased linearly up to limited concentrations for both samples (about 1.0 μg/mL), as shown in Figure 5A. Above that concentration, further addition of protein did not result in a further increase of area in the UV−vis spectra in either of the cases. However, for the samples consisting of denatured protein, significant precipitation could be observed at above the concentration of 1.07 μg/mL, leading to a loss of absorption intensity. Interestingly, the trends in the slopes of the areas corresponding to AMG were different from those of samples with α-amylase and GFP. For example, the slope of the area versus concentration plot of the NPs in the presence of denatured protein is much steeper and closer to the slope of the native form (Figure 5B). Also, changes in the area of the graphs were more significant than those with the denatured forms of α-amylase and GFP. The concentrations of the protein at which the values of the saturations were reached were also much higher in comparison to the other two proteins. The results indicate that interactions of protein with Au NPs depend strongly on its three-dimensional conformation as well as the groups that are exposed to the medium. Experimental observations suggest that the interactions of Au NPs with proteins having exposed thiol groups are different from those of nonthiol containing proteins. Further, Lorentzian fit of the absorption spectra of Au NPs in the presence of different concentrations of native and denatured protein indicate that in addition to the peak due to unagglomerated NPs, a second peak appeared, the intensity of which increased with increasing concentrations of both forms of protein (Figure S10 of the Supporting Information). Also, the original peak due to unagglomerated Au NPs decreased gradually in area with the amount of protein. Plots of the areas of both types of peak indicate clearly the agglomeration of the NPs in the presence of proteins—both in native and denatured forms (Figure 5C,D). Further, the trends in changes in the areas of the deconvoluted absorption spectra—i.e., summation of the areas of the two graphs—matched well with the experimental observations. Overall, the observations indicated that for AMG, the denatured form of the protein led to agglomeration of NPs much more than that due to the denatured form of other two proteins (α-amylase and GFP). Interestingly, the denatured form led to more agglomeration than its native form, in comparison to the other two proteins.

Further, addition of BSA to Au NPs exhibited results although apparently similar to the above enzymes but there were also fundamental differences from the others. For example, addition of both the native and denatured form of proteins led to broadening of the spectra. However, broadening and shifts of the peaks due to addition of denatured form were much more prominent than the native form of the protein (Figure S11 of the Supporting Information). These results are similar to those of AMG but very different from the other two proteins (α-amylase and GFP) used herein. Plots of area versus concentration of native as well as denatured protein (Figure 6A,B) showed that the changes associated with addition of both forms of the protein were prominent; however, the slope of the graphs for the denatured one was much more steep than that

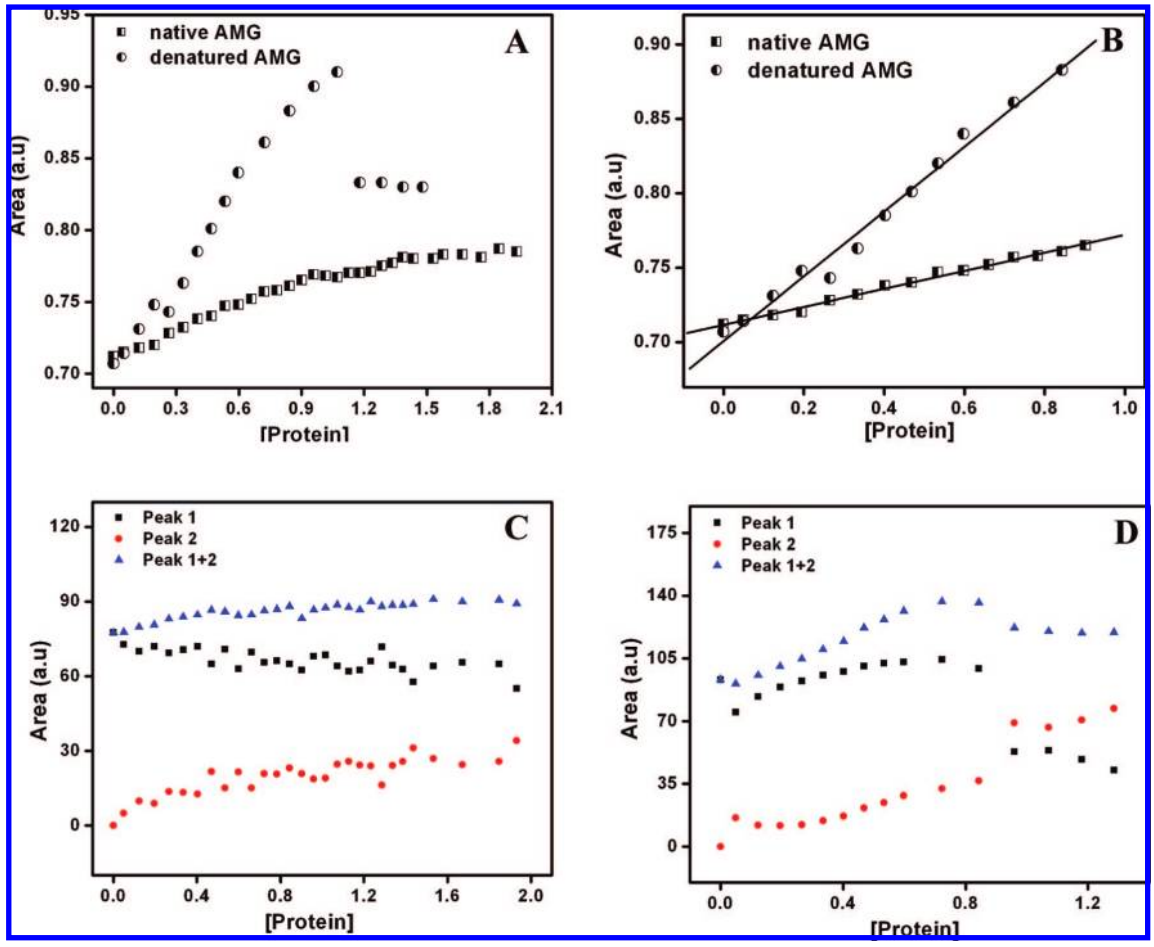

Figure 5. (A) Area under the graph versus the corresponding protein concentration (in μg/mL) for native and denatured AMG. (B) The linear region of the graphs in A. The peak areas of all the component peaks and their summation against the protein concentration (in μg/mL) obtained by deconvolution for (C) native AMG and (D) denatured AMG.

with the native protein—in the linear region of the graphs. The linearity was valid up to a concentration of 1.639 μg/mL for both forms of the protein. Further, agglomeration of the NPs in the presence of both native and denatured forms of the protein was substantiated by TEM measurements (Figure S12 of the Supporting Information). Deconvolutions of the absorption spectra (Figure S13 of the Supporting Information) indicated that the best fits were obtained with three curves (in addition to the background)—one for the peak due to unagglomerated Au NPs, while the other two are due to agglomerated composites. The intensity of the peak due to Au NPs (unagglomerated) decreased with the addition of proteins, whereas two more peaks appeared simultaneously. The total area due to three peaks matched well with the experimentally observed area versus protein concentration plot. This was valid for both forms of the protein. It is plausible that agglomeration of Au NPs in the presence of BSA follows a different path from the other three enzymes. It might also be true that there are two kinds of agglomeration; one where the peak shift is less and the change may be due to the change of dielectric constants and agglomeration similar to the other proteins. However, the peak at the higher wavelength could be due to strong interplasmon resonance coupling between the NPs and thus occur at higher wavelengths. This peak represents the agglomeration of Au NPs in the presence of the protein, which is specific to BSA. However, fundamentally, the results indicate different level of agglomeration in the presence of different proteins and their conformational states. Thus the present method not only provides a new way of estimating the protein concentration in a medium, but also brings out evidence of interaction specific to its nature and conformation in solution.

The results obtained with respect to the effect of four proteins on the UV−vis spectra of Au NPs are summarized in Table 1 and Table 2. Table 1 indicates the detection limit achieved using the present method of finding protein concentrations and absolute amount in solution, for all four of them in both their native and denatured forms. Similarly, the results of the deconvolution analyses of the UV−vis spectra of Au NPs in the presence of all four proteins are shown in Table 2. The results essentially show that the detection limit of protein concentration is dependent on the nature of the protein with its three-dimensional conformation. The method is most sensitive to the detection of native α-amylase as the lowest concentration that can be detected is 2.0 ng/mL, the absolute amount used here being 6 ng. Interestingly, the denatured form leads to detection of the lowest concentration at 20 ng/mL, which is higher than that of the native form. The next lowest limit is for AMG (both in native and denatured forms) with a value of 50 ng/mL. The lowest limits for GFP and BSA were identical and the value was 330 ng/mL for both the native and denatured forms. However, the highest concentrations of the proteins that can be detected using the present method followed the same trend as those of the lowest limits. This is reasonable considering that the detection limits fall in the linear regimes of variation of absorbance with concentration of protein. Further, as is clear from Table 2, the Lorentzian fit of the absorption spectra for

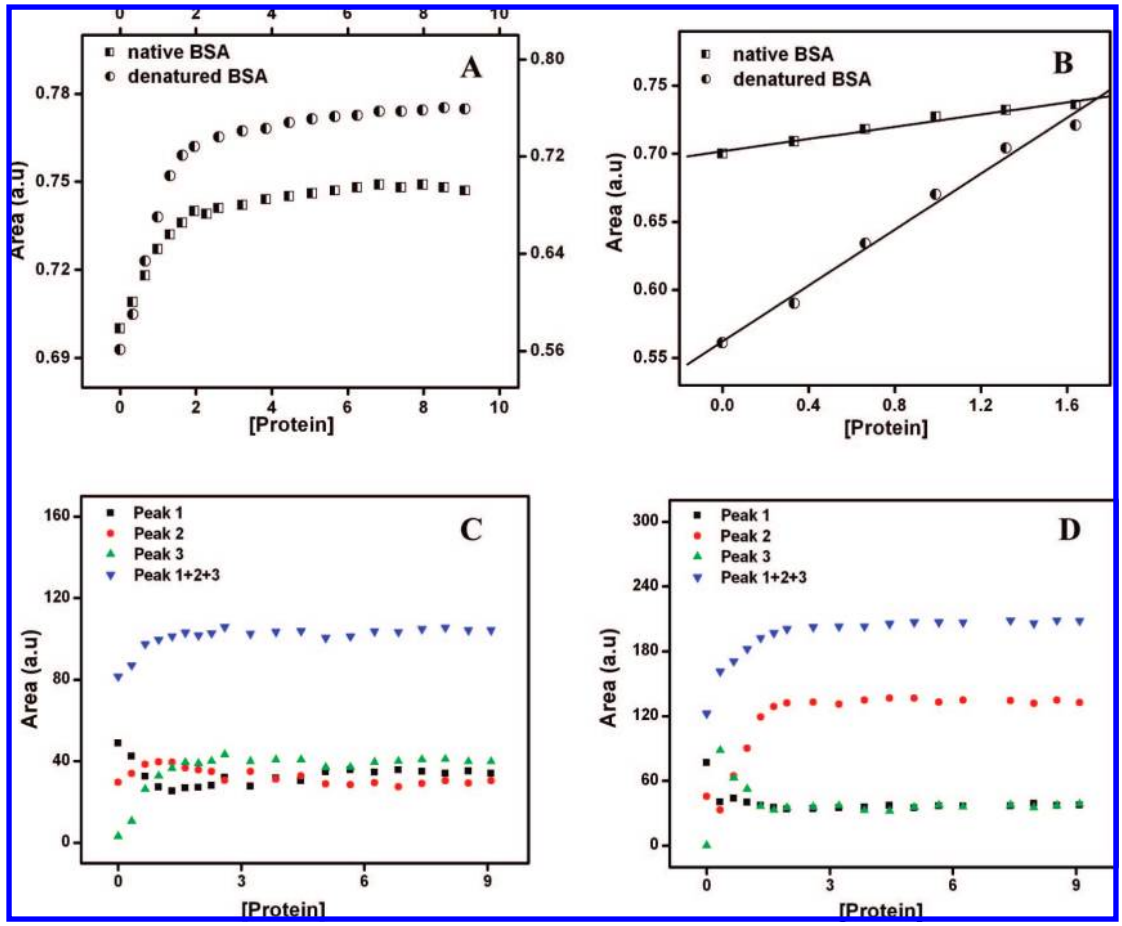

Figure 6. (A) Area under the graph versus the corresponding protein concentration for native and denatured BSA (the left Y-axis is for native BSA and right Y-axis for denatured BSA) (B) The linear region of the graphs in A. The peak areas of all the component peaks and their summation against the protein concentration (in μg/mL) obtained by deconvolution for (C) native BSA and (D) denatured BSA.

TABLE 1: Experimental Results of the Sensitivity Range of Protein Detection

sl. no.	enzyme/protein	sensitivity range of protein detection	
		μg/mL of protein (lower−upper limit)	μg of protein (lower−upper limit)
1	amylase−native	0.002−0.100	0.006−0.330
2	amylase−denatured	0.02−0.34	0.06−1.14
3	GFP−native	0.33−1.64	1.00−5.00
4	GFP−denatured	0.33−3.85	1.00−12.00
5	AMG−native	0.05−0.96	0.15−3.30
6	AMG−denatured	0.05 − 0.90	0.15−3.07
7	BSA−native	0.33−1.64	1.00−5.00
8	BSA−denatured	0.33−1.64	1.00−5.00

TABLE 2: Details of Component Peaks for All Sets of Enzyme/Protein Used and As Obtained from Deconvolution of the SPR Peaks

sl. no.	enzyme/protein	no. of peaks	peak shift (in nm)		
			peak 1 (nm)	peak 2 (nm)	peak 3 (nm)
1	amylase−native	02	const. at 522	542−572	nil
2	amylase−denatured	01	const. at 522	nil	nil
3	GFP−native	02	const. at 522	542−572	nil
4	GFP−denatured	02	const. at 522	542−572	nil
5	AMG−native	02	const. at 522	542−562	nil
6	AMG−denatured	02	const. at 522	542−572	nil
7	BSA−native	03	const. at 522	542−572	572−583
8	BSA−denatured	03	const. at 522	542−572	562−644

different proteins revealed that typically, appearance of an additional peak (other than the original absorption due to unagglomerated Au NPs) is sufficient to account for the change in spectral characteristics of the spectra upon addition of proteins of different concentration. The second peak position appears at 542 nm and continuously changes until it reaches 572 nm in the linear regimes. This could possibly indicate the level of agglomerations of proteins with Au NPs which increases with protein concentration, giving rise to continuous change in dielectric constant and hence peak positions. The above results were found to be true for α-amylase (native form only), GFP and AMG. However, the denatured α-amylase form did not have

a second peak indicating that there was no agglomeration; the change in intensity could be accounted for by the change in dielectric constant upon addition of the protein. Interestingly, in order to fit the absorption spectra due to BSA two additional peaks were required. The appearance and behavior of the first one was similar to those of the other proteins. The third peak appeared at a higher wavelength in the region of 572−584 nm for the native form and 562−644 nm for the denatured form. This clearly indicates a second process of agglomeration for both forms of the protein and effect of the native form is different from that due to denatured form.

It is clear from the above results that the way a particular enzyme/protein interacts with citrate-capped Au NP is specific to its nature as well its three-dimensional conformation. The protein specific interaction gives rise to different broadening in the absorption spectra, which depends on the nature and level of agglomeration of the composite of protein and citrate-capped NPs. Also, since the protein detection range differs from protein to protein, hence the way a protein interacts must be specific to its 3D conformation with the presence (and absence) of various amino acid residues which could interact with Au NPs leading to different consequent structures (agglomeration). The observation that the detection limit for native state of α-amylase being the lowest clearly indicates the role of free and exposed thiol groups present in the native structures of the proteins. However, since the results with GFP are different, it can be concluded that a free and exposed thiol group alone does not play the key role in the change of absorbance characteristics of Au NPs. In other words, the amino acid residues other than those containing free and exposed thiols also play critical roles in the agglomeration of Au NPs in the presence of protein and subsequent effect on the spectra behavior of Au NPs. This is all the more clear from the detection limits of AMG (both forms of the protein) being much lower than those of GFP. Also, the proteins attached to the NPs may facilitate agglomeration, which could be different for different proteins, leading to variation of the point of saturation in the absorption spectra. However, when the thiol groups in the denatured proteins may not be exposed to the solution, the affinity for binding to the NPs may be different and hence the changes in the absorption spectra would occur at a protein concentration different from that of the native form; which may be driven primarily by electrostatic interactions involving other amino acid residues. For example, AMG and BSA, both of which lack free thiol groups on their surfaces in their native state, may interact with the Au NPs via the amino acid residues electrostatically only. This possibly occurs at higher concentrations of proteins and thus the higher detection limit. Interestingly, on being denatured, the buried free thiol group of the BSA might not necessarily be available to bring any change in the detection range of protein as has been observed experimentally. However, the detection limits for BSA and AMG being significantly different indicates that the nature of interactions between proteins and citrate-stabilized Au NPs may be more complex that to be explained based on simple electrostatic interactions involving the amino acid residues. For example, the proteins upon being adsorbed on the NP surface may interact with other protein (present in other NP) very differently than that between two free proteins in solution and may give rise to more complicated interactions.

Finally, it may be mentioned here that the changes in the spectral characteristics of Au NPs may not be absolute with respect to addition of proteins. In other words, the exact changes in the spectra may vary depending on the sizes of the NPs and their distribution. However, in general, NPs can be produced with reproducible sizes and their distribution with unique spectra, especially in the presence of stabilizers. We have observed that under the same reaction conditions, the UV−vis absorption spectra of Au NPs produced from different batch could be superimposed. Thus, the present method should provide reproducible results. However, in the event of NPs not being produced with predictable sizes and the UV−vis spectra of protein free Au NPs varying from sample to sample, a calibration curve could be obtained (with the protein and its concentration), which should be sufficient for identification and estimation of samples of unknown concentration and nature of protein following the above method. Further, it is important to mention here that in order for the method to be robust there should be no time-dependence of the UV−vis spectra of the Au NPs upon addition of various amounts of proteins. As any such dependence would indicate secondary interactions and subsequent calculations of the concentrations from the changes in the area of the graph would then be erroneous. To probe this, we have recorded the time-dependent UV−vis spectra of Au NPs after addition of native amylase, native and denatured BSA. The results indicate that there is hardly any time-dependence in the peak of the Au NPs after addition of various amounts of proteins. Also, there is no substantial change in the area versus concentration plots with time for the above proteins. The corresponding time-dependent UV−vis spectra and area versus protein concentration plots are shown in the Supporting Information (Figures S14−S16).

Conclusions

The series of experiments performed with four different enzymes/proteins have demonstrated a versatile, simple, and rapid method of protein assay in solution using optical absorption changes of citrate-stabilized Au NPs, which can be performed at room temperature and in both the native and denatured conformations of the proteins. The additional advantage of the method lies in its ability to distinguish between the native and denatured conformation of a particular enzyme/protein, in conjunction with the estimation of the amount of protein. The method relies on the interaction of the protein with citrate stabilized Au NPs leading to the changes in the absorption spectra due to the NPs. At low concentrations, replacement of the citrate capping by the proteins led to broadening of the spectrum. Alternatively, at higher concentrations, a second peak due to agglomeration of the NPs in the presence of protein appears which leads to further broadening of the spectrum. The method at present is applicable to pure proteins as the presence of interfering agents may lead to different results. The method is superior in comparison to conventional methods in terms of its ability to not only estimate low concentrations of protein rapidly but also distinguish the native conformations from the denatured one. The present work could lead to further understanding about the interactions between a protein and Au NPs and activity of the enzyme in the presence of the NPs, which we are currently pursuing. Finally, this simple and possibly general method may pave the way for the development of more versatile methods of protein and other biomolecule assays even in vivo.

Acknowledgment. We thank the Department of Science and Technology, (DST Nos. SR/S5/NM-01/2005 and 2/2/2005-S.F), Council of Scientific and Industrial Research (01(2172)/07/EMR-II)), and Department of Biotechnology (BT/PR9988/NNT/28/76/2007), Government of India for financial support. J.D. thanks CSIR for a fellowship. We also thank Pallab Sanpui for providing GFP.

Supporting Information Available: DLS-based particle size analysis results, additional UV−vis spectra and their analyses, and additional TEM images are available. This material is available free of charge via the Internet at http://pubs.acs.org.

References and Notes

(1) Sarikaya, M. *Proc. Natl Acad Sci. U.S.A.* **1999**, *96*, 14183.

(2) Seeman, N. C.; Belcher, A. M. *Proc. Natl Acad Sci. U.S.A.* **2002**, *99*, 6452.

(3) Ball, P. *Nature* **2001**, *409*, 413.

(4) Hye, A.; Lynham, S.; Thambisetty, M.; Causevic, M.; Campbell, J.; Byers, H. L.; Hooper, C.; Rijsdijk, F.; Tabrizi, S. J.; Banner, S.; Shaw, C. E.; Foy, C.; Poppe, M.; Archer, N.; Hamilton, G.; Powell, J.; Brown, R. G.; Sham, P.; Ward, M.; Lovestone, S. *Brain* **2006**, *129*, 3042.

(5) Hanash, S. *Nature* **2003**, *422*, 226.

(6) Srinivas, P. R.; Srivastava, S.; Hanash, S.; Wright, G.L.Jr. *Clin. Chem.* **2001**, *47* (10), 1901.

(7) Dunn, M. J. *Therapeut. Focus* **2000**, *5* (2), 76.

(8) http://www.rcsb.org.

(9) Shipway, A. N.; Katz, E.; Willner, I. *ChemPhysChem* **2000**, *1*, 18.

(10) Portney, N. G.; Ozkan, M. *Anal. Bioanal. Chem.* **2006**, *384*, 620.

(11) West, J. L.; Halas, N. J. *Ann. Rev. Biomed. Eng.* **2003**, *5*, 285.

(12) Li, C. Z.; Liu, Y.; Luong, J. H. T *Anal. Chem.* **2005**, *77* (2), 478.

(13) Jain, K. K *Expert Rev. Mol. Diagn.* **2003**, *3* (2), 153.

(14) Storhoff, J. J.; Elghanian, R.; Mucic, R. C.; Mirkin, C. A.; Letsinger, R. L. *J. Am. Chem. Soc.* **1998**, *120* (9), 1959.

(15) Hone, D. C.; Haines, A. H.; Russell, D. A. *Langmuir* **2003**, *19*, 7141.

(16) Mayer, K. M.; Lee, S.; Liao, H.; Rostro, B. C.; Fuentes, A.; Scully, P. T.; Nehl, C. L.; Hafner, J. H. *ACS Nano* **2008**, *2* (4), 687.

(17) Chen, Y. M.; Yu, C. J.; Tseng, W. L. *Langmuir* **2008**, *24* (7), 3654.

(18) Casanova, D.; Giaume, D.; Moreau, M.; Martin, J. L.; Gacoin, T.; Boilot, J. P.; Alexandrou, A. *J. Am. Chem. Soc.* **2007**, *129* (42), 12592.

(19) Hirsch, L. R.; Jackson, J. B.; Lee, A.; Halas, N. J.; West, J. L. *Anal. Chem.* **2003**, *7* (10), 2377.

(20) Soman, C. P.; Giorgio, T. D. *Langmuir* **2008**, *24* (8), 4399.

(21) Mahmoud, K. A.; Hrapovic, S.; Luong, J. H. T. *ACS Nano* **2008**, *2* (5), 1051.

(22) Tsai, C. S.; Yu, T. B.; Chen, C. T. *Chem. Commun.* **2005**, 4273.

(23) Bayraktar, H.; Ghosh, P. S.; Rotello, V. M.; Knapp, M. J. *Chem. Commun.* **2006**, 1390.

(24) Baciu, C. L.; Becker, J.; Janshoff, A.; Sonnichsen, C. *Nano Lett.* **2008**, *8* (6), 1724.

(25) Bao, J.; Chen, W.; Liu, T.; Zhu, Y.; Jin, P.; Wang, L.; Liu, J.; Wei, Y.; Li, Y *ACS Nano* **2007**, *1* (4), 293.

(26) Chah, S.; Kumar, C. V.; Hammond, M. R.; Zare, R. N. *Anal. Chem.* **2004**, *76* (7), 2112.

(27) Chah, S.; Hammond, M. R.; Zare, R. N. *Chem. Biol.* **2005**, *12*, 323.

(28) Shang, L.; Wang, Y.; Jiang, J.; Dong, S. *Langmuir* **2007**, *23*, 2714.

(29) Harrison, G.; Haffey, P.; Golub, E. E. *Anal. Biochem.* **2008**, *380* (1), 1.

(30) Moeremans, M.; Daneels, G.; Mey, J. D. *Anal. Biochem.* **1985**, *145*, 315.

(31) Stoscheck, C. M. *Anal. Biochem.* **1987**, *160*, 301.

(32) Brewer, S. H.; Glomm, W. R.; Johnson, M. C.; Knag, M. K.; Franzen, S. *Langmuir* **2005**, *21*, 9303.

(33) Winkles, J.; Lunec, J.; Deverill, I. *Clin. Chem.* **1987**, *33* (5), 685–689.

(34) Dykman, L. A.; Bogatyrev, V. A.; Khlebtsov, B. N.; Khlebtsov, N. G. *Anal. Biochem.* **2005**, *341*, 16–21.

(35) Grabar, K. C.; Freeman, R. G.; Hommer, M. B.; Natan, M. *J. Anal. Chem.* **1995**, *67*, 735.

(36) Frens, G. *Nat. Phys. Sci.* **1973**, *241*, 20.

(37) Sanpui, P.; Pandey, S. B.; Ghosh, S. S.; Chattopadhyay, A. *J. Colloid Interface Sci.* **2008**, *326* (1), 129.

(38) Bradford, M. M. *Anal. Biochem.* **1976**, *72*, 248.

(39) Zor, T.; Selinger, Z. *Anal. Biochem.* **1996**, *236*, 302.

(40) Mulvaney, P. *Langmuir* **1996**, *12*, 788.

(41) Sato, K.; Hosokawa, K.; Maeda, M. *J. Am. Chem. Soc.* **2003**, *125*, 8102.

(42) Zhao, W.; Chiuman, W.; Lam, J. C. F.; Brook, M. A.; Li, Y. *Chem. Commun.* **2007**, 3729.

(43) Rangnekar, A.; Sarma, T. K.; Singh, A. K.; Deka, J.; Ramesh, A.; Chattopadhyay, A *Langmuir* **2007**, *23* (10), 5700.

(44) Deka, J.; Paul, A.; Ramesh, A.; Chattopadhyay, A *Langmuir* **2008**, *24* (18), 9945.

JP808405P